Diamagnetically stabilized magnet levitation

M. D. Simon, Department of Physics and Astronomy,
University of California, Los Angeles
L. O. Heflinger, Torrance CA, and A. K. Geim,
Department of Physics and Astronomy, University of Manchester, UK
contact msimon@physics.ucla.edu

Manuscript number 12096, March. 29, 2001

Abstract

Stable levitation of one magnet by another with no energy input is usually prohibited by Earnshaw's Theorem. However, the introduction of diamagnetic material at special locations can stabilize such levitation. A magnet can even be stably suspended between (diamagnetic) fingertips. A very simple, surprisingly stable room temperature magnet levitation device is described that works without superconductors and requires absolutely no energy input. Our theory derives the magnetic field conditions necessary for stable levitation in these cases and predicts experimental measurements of the forces remarkably well. New levitation configurations are described which can be stabilized with hollow cylinders of diamagnetic material. Measurements are presented of the diamagnetic properties of several samples of bismuth and graphite.

1 Diamagnetic materials

Most substances are weakly diamagnetic and the tiny forces associated with this property make two types of levitation possible. Diamagnetic materials, including water, protein, carbon, DNA, plastic, wood, and many other common materials, develop persistent atomic or molecular currents which

oppose externally applied magnetic fields. Bismuth and graphite are the elements with the strongest diamagnetism, about 20 times greater than water. Even for these elements, the magnetic susceptibility χ is exceedingly small, $\chi \approx -170 \times 10^{-6}$.

In the presence of powerful magnets the tiny forces involved are enough to levitate chunks of diamagnetic materials. Living things mostly consist of diamagnetic molecules (such as water and proteins) and components (such as bones). Contrary to our intuition, these apparently nonmagnetic substances, including living plants and small animals, can be levitated in a magnetic field [1, 2].

Diamagnetic materials can also stabilize free levitation of a permanent magnet which is the main subject of this paper. This approach can be used to make very stable permanent magnet levitators that work at room temperature without superconductors and without energy input. Recently, levitation of a permanent magnet stabilized by the diamagnetism of human fingers ($\chi \approx -10^{-5}$) was demonstrated at the High Field Magnet Lab in Nijmegen, The Netherlands [3, 4].

While the approximate magnitude of the diamagnetic effect can be derived from simple classical arguments about electron orbits, diamagnetism is impossible within classical physics. The Bohr-Leeuwen Theorem states that no properties of a classical system in thermal equilibrium can depend in any way on the magnetic field [5, 6]. In a classical system, at thermal equilibrium the magnetization must always vanish. Diamagnetism is a macroscopic manifestation of quantum physics that persists at high temperatures, $kT \gg \mu_{Bohr}B$.

2 Earnshaw's Theorem

Those who have studied levitation, charged particle traps, or magnetic field design for focusing magnets have probably run across Earnshaw's theorem and its consequences. There can be no purely electrostatic levitator or particle trap. If a magnetic field is focusing in one direction, it must be defocusing in some orthogonal direction. As students, most of us are asked to prove the electrostatic version which goes something like this: Prove that there is no configuration of fixed charges and/or voltages on fixed surfaces such that a test charge placed somewhere in free space will be in stable equilibrium. It is easy to extend this proof to include electric and magnetic dipoles.

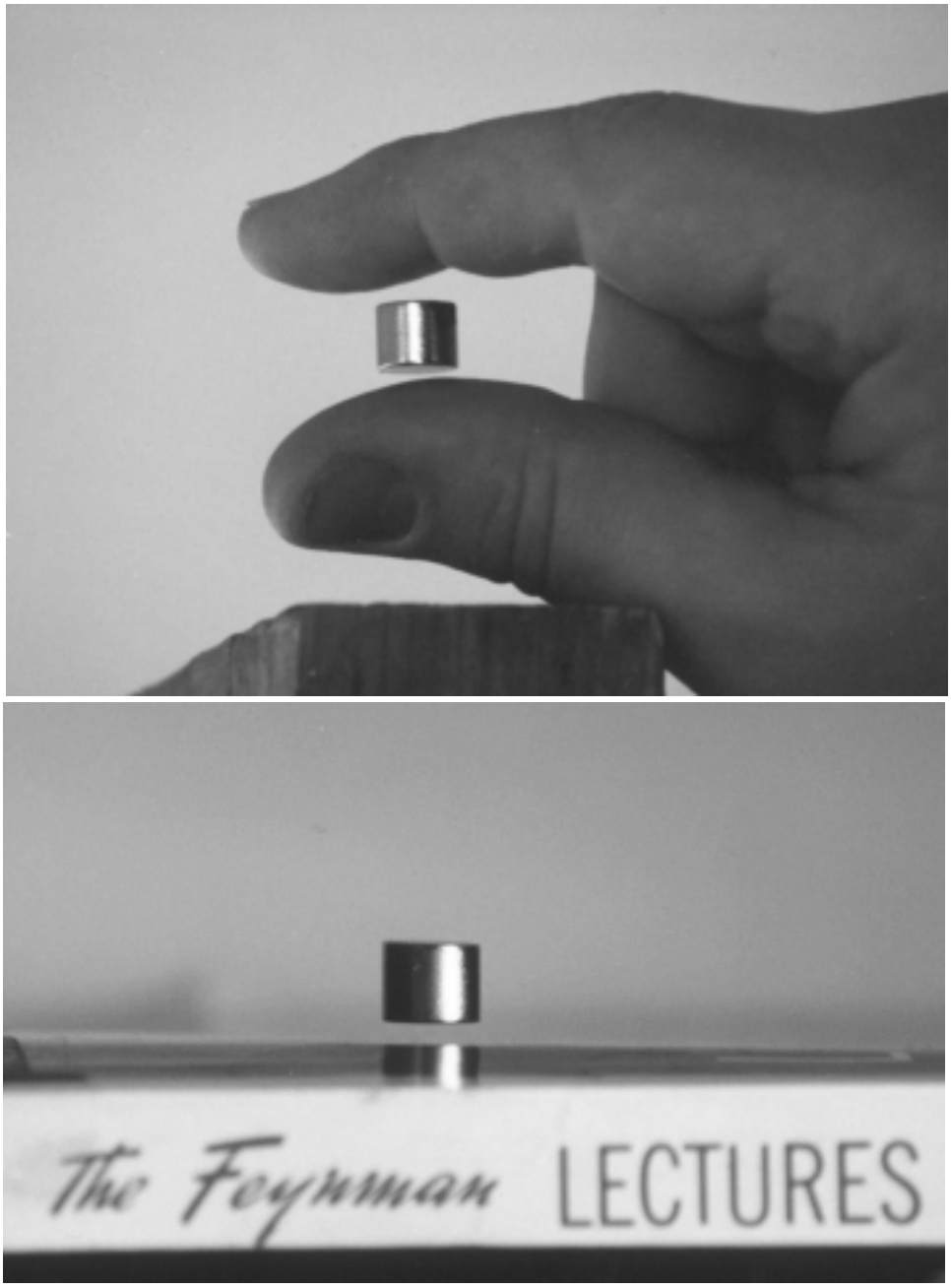

Figure 1: *top:* Levitation of a magnet 2.5 m below an unseen 11 T superconducting solenoid stabilized by the diamagnetism of fingers ($\chi \approx -10^{-5}$). *bottom:* Demonstrating the diamagnetism of our favorite text explaining diamagnetism.

It is useful to review what Earnshaw proved and the consequences for physics. As can be seen from the title of Earnshaw's paper [7], "On the nature of the molecular forces which regulate the constitution of the luminiferous ether", he was working on one of the frontier physics problems of his time (1842). Earnshaw wrote before Maxwell's work, before atoms were known to be made up of smaller particles, and before the discovery of the electron. Scientists were trying to figure out how the ether stayed uniformly spread out (some type of repulsion) and how it could isotropically propagate the light disturbance.

Earnshaw discovered something simple and profound. Particles in the ether could have no stable equilibrium position if they interacted by any type or combination of $1/r^2$ forces. Most of the forces known such as gravity, electrostatics, and magnetism are $1/r^2$ forces. Without a stable equilibrium position (and restoring forces in all directions), ether particles could not isotropically propagate wavelike disturbances. Earnshaw concluded that the ether particles interacted by other than $1/r^2$ forces. Earnshaw's paper torpedoed many of the popular ether theories of his time.

Earnshaw's theorem depends on a mathematical property of the $1/r$ type energy potential. The Laplacian of any sum of $1/r$ type potentials is zero, or $\nabla^2 \ \Sigma k_i/r = 0$. This means that at any point where there is force balance ($-\nabla \ \Sigma k_i/r = 0$), the equilibrium is unstable because there can be no local minimum in the potential energy. Instead of a minimum in three dimensions, the energy potential surface is a saddle. If the equilibrium is stable in one direction, it is unstable in an orthogonal direction.

Since many of the forces of nature are $1/r^2$ forces, the consequences of Earnshaw's theorem go beyond the nature of the ether. Earnshaw understood this himself and writes that he could have titled his paper "An Investigation of the Nature of the Molecular Forces which regulate the Internal Constitution of Bodies". We can be sure that when J. J. Thomson discovered the electron fifty-five years later, he considered Earnshaw's theorem when he proposed the plum pudding model of atoms. Thomson's static model avoided $1/r^2$ forces by embedding the electrons in a uniform positive charge. In this case the energy obeys Poisson's equation rather than LaPlace's. Rutherford's scattering experiments with Geiger and Marsden in 1910 soon showed that the positive charge was concentrated in a small massive nucleus and the problem of atomic structure was not solved until Bohr and quantum mechanics.

Earnshaw's theorem applies to a test particle, charged and/or a magnet,

located at some position in free space with only divergence- and curl-free fields. No combination of electrostatic, magnetostatic, or static gravitational forces can create the three-dimensional potential well necessary for stable levitation in free space. The theorem also applies to any array of magnets or charges.

An equivalent way to look at the magnetic case is that the energy U of a magnetic dipole $\mathbf{M}$ in a field $\mathbf{B}$ is

$$U = -\mathbf{M} \cdot \mathbf{B} = -M_x B_x - M_y B_y - M_z B_z. \tag{1}$$

If $\mathbf{M}$ is constant the energy depends only on the components of $\mathbf{B}$. However, for magnetostatic fields,

$$\boldsymbol{\nabla}^2 \mathbf{B} = 0 \tag{2}$$

and the Laplacian of each component is zero in free space and so $\boldsymbol{\nabla}^2 U = 0$ and there is no local energy minimum.

At first glance, any static magnetic levitation appears to contradict Earnshaw's theorem. There must be some loopholes though, because magnets above superconductors, the spinning magnet top, diamagnets including living things, and the magnet configurations to be described here do stably levitate.

3 Beyond Earnshaw

Earnshaw's theorem does not consider magnetic materials except for hard fixed magnets. Ferro- and paramagnetic substances align with the magnetic field and move toward field maxima. Likewise, dielectrics are attracted to electric field maxima. Since field maxima only occur at the sources of the field, levitation of paramagnets or dielectrics in free space is not possible. (An exception to this statement is when a paramagnet is made to behave like a diamagnet by placing it in a stronger paramagnetic fluid. Bubbles in a dielectric fluid act in a similar way. A second exception is when isolated local maxima are created by focusing an AC field as with laser tweezers [8].)

Paramagnets and diamagnets are dynamic in the sense that their magnetization changes with the external field. Diamagnets are repelled by magnetic fields and attracted to field minima. Since local minima can exist in free space, levitation is possible for diamagnets. We showed above that there are no local minima for any vector component of the magnetic field. However there can be local minima of the field magnitude.

Soon after Faraday discovered diamagnetic substances, and only a few years after Earnshaw's theorem, Lord Kelvin showed theoretically that diamagnetic substances could levitate in a magnetic field [9]. In this case the energy depends on $B^2 = \mathbf{B} \cdot \mathbf{B}$ and the Laplacian of B^2 can be positive. In fact [1, 8]

$$\boldsymbol{\nabla}^2 \; B^2 \geq 0. \tag{3}$$

The key idea here and in the levitation schemes to follow, the way around Earnshaw's theorem, is that the energy is not linearly dependent on the individual components of $\mathbf{B}$. The energy is dependent on the magnitude B. Three-dimensional minima of individual components do not exist. For static fields, local maxima of the field magnitude cannot exist in free space away from the source of the field. However, local minima of the field magnitude can exist.

Braunbek [10] exhaustively considered the problem of static levitation in 1939. His analysis allowed for materials with a dielectric constant ϵ and permeability μ different than 1. He showed that stable static levitation is possible only if materials with $\epsilon < 1$ or $\mu < 1$ are involved. Since he believed there are no materials with $\epsilon < 1$, he concluded that stable levitation is only possible with the use of diamagnetic materials.

Braunbek went further than predicting diamagnetic levitation. He figured out the necessary field configuration for stable levitation of a diamagnet and built an electromagnet which could levitate small specks of diamagnetic graphite and bismuth [10]. With the advent of powerful 30 Tesla magnets, even a blob of water can now be levitated.

Superconducting levitation, first achieved in 1947 by Arkadiev [11], is consistent with Braunbek's theory because a superconductor acts like a perfect diamagnet with $\mu = 0$. Flux pinning in Type II superconductors adds some complications and can lead to attractive as well as repulsive forces.

The only levitation that Braunbek missed is spin-stabilized magnetic levitation of a spinning magnet top over a magnet base which was invented by Roy Harrigan [12]. Braunbek argued that if a system is unstable with respect to translation of the center of mass, it will be even more unstable if rotations are also allowed. This sounds reasonable but we now know that imparting an initial angular momentum to a magnetic top adds constraints which have the effect of stabilizing a system which would otherwise be translationally unstable [13, 14]. However, this system is no longer truly static though once set into motion, tops have been levitated for 50 hours in high vacuum with

Material	$-\chi$ ($\times 10^{-6}$)
water	8.8
gold	34
bismuth metal	170
graphite rod	160
pyrolytic gr. $\perp$	450
pyrolytic gr. $\parallel$	85

Table 1: Values of the dimensionless susceptibility χ in SI units for some diamagnetic materials. The measurement method for the graphites is discussed in a later section.

no energy input [15].

The angular momentum and precession keep the magnet top aligned antiparallel with the local magnetic field direction making the energy dependent only on the magnitude $|\mathbf{B}| = [\mathbf{B} \cdot \mathbf{B}]^{1/2}$. Repelling spinning dipoles can be levitated near local field minima. Similar physics applies to magnetic gradient traps for neutral particles with a magnetic moment due to quantum spin [16]. The diamagnetically stabilized floating magnets described below stay aligned with the local field direction and also depend only on the field magnitude.

4 Magnet Levitation with Diamagnetic Stabilization

We know from Earnshaw's theorem that if we place a magnet in the field of a fixed lifter magnet where the magnetic force balances gravity and it is stable radially, it will be unstable vertically. Boerdijk (in 1956) used graphite below a suspended magnet to stabilize the levitation [17]. Ponizovskii used pyrolytic graphite in a configuration similar to the vertically stabilized levitator described here [18]. As seen in table I, the best solid diamagnetic material is pyrolytic graphite which forms in layers and has an anisotropic susceptibility (and thermal conductivity). It has much higher susceptibility perpendicular to the sheets than parallel.

It is also possible to levitate a magnet at a location where it is stable vertically but unstable horizontally. In that case a hollow diamagnetic cylinder

can be used to stabilize the horizontal motion [3, 4].

The potential energy U of a floating magnet with dipole moment $\mathbf{M}$ in the field of the lifter magnet is,

$$U = -\mathbf{M} \cdot \mathbf{B} + mgz \; = \; -MB + mgz. \tag{4}$$

where mgz is the gravitational energy. The magnet will align with the local field direction because of magnetic torques and therefore the energy is only dependent on the magnitude of the magnetic field, not any field components.

Taking advantage of the irrotational and divergenceless nature of magnetostatic fields in free space, we can expand the field around the levitation point in terms of the primary field direction, here B_z, and its derivatives.

$$B_z = B_0 + B'z + \frac{1}{2}B''z^2 - \frac{1}{4}B''(x^2 + y^2) + \cdots \tag{5}$$

$$\begin{aligned} B_x &= -\frac{1}{2}B'x - \frac{1}{2}B''xz + \cdots \\ B_y &= -\frac{1}{2}B'y - \frac{1}{2}B''yz + \cdots \end{aligned} \tag{6}$$

where

$$B' = \frac{\partial B_z}{\partial z}, \text{ and } B'' = \frac{\partial^2 B_z}{\partial z^2} \tag{7}$$

and the derivatives are evaluated at the levitation point.

For a cylindrically symmetric geometry we expand around the B_z component and its derivatives.

$$B_z = B_0 + B'z + \frac{1}{2}B''z^2 - \frac{1}{4}B''r^2 + \cdots \tag{8}$$

$$B_r = -\frac{1}{2}B'r - \frac{1}{2}B''rz + \cdots \tag{9}$$

Then

$$B^2 = B_0^2 + 2B_0B'z + \{B_0B'' + B'^2\}z^2 + \frac{1}{4}\{B'^2 - 2B_0B''\}r^2 + \cdots \tag{10}$$

where $r^2 = x^2 + y^2$.

Expanding the field magnitude of the lifter magnet around the levitation point using equations 7, 8, and 9 and adding two new terms C_zz^2 and C_rr^2

which represent the influence of diamagnets to be added and evaluated next, the potential energy of the floating magnet is

$$U = -M\Big[B_0 + \Big\{B' - \frac{mg}{M}\Big\}z + \frac{1}{2}B''z^2 + \frac{1}{4}\Big\{\frac{B'^2}{2B_0} - B''\Big\}r^2 + \cdots\Big] + C_z z^2 + C_r r^2 \tag{11}$$

At the levitation point, the expression in the first curly braces must go to zero. The magnetic field gradient balances the force of gravity

$$B' = \frac{mg}{M} \tag{12}$$

The conditions for vertical and horizontal stability are

$$K_v \equiv C_z - \frac{1}{2}MB'' > 0 \quad \text{vert. stability} \tag{13}$$

$$K_h \equiv C_r + \frac{1}{4}M\Big\{B'' - \frac{B'^2}{2B_0}\Big\} = C_r + \frac{1}{4}M\Big\{B'' - \frac{m^2g^2}{2M^2B_0}\Big\} > 0 \quad \text{hor. stability} \tag{14}$$

Without the diamagnets, setting $C_r = 0$ and $C_z = 0$, we see that if $B'' < 0$ creating vertical stability, then the magnet is unstable in the horizontal plane. If the curvature is positive and large enough to create horizontal stability, then the magnet is unstable vertically.

We consider first the case where $B'' > 0$ and is large enough to create horizontal stability $K_h > 0$. The top of figure 2 shows plots of K_v and K_h for the case of a ring magnet lifter. The dashed line shows the effect of the C_z term. Where both curves are positive, stable levitation is possible if $MB' = mg$. It is possible to adjust the gradient or the weight of the floating magnet to match this condition.

We can see that there are two possible locations for stable levitation, one just below the field inflection point where B'' is zero and one far below the lifter magnet where the fields are asymptotically approaching zero. The upper position has a much stronger gradient than the lower position. The lower position requires less diamagnetism to raise K_v to a positive value and the stability conditions can be positive over a large range of gradients and a large spatial range. This is the location where fingertip stabilized levitation is possible. It is also the location where the magnet in the compact levitator of figure 4 floats.

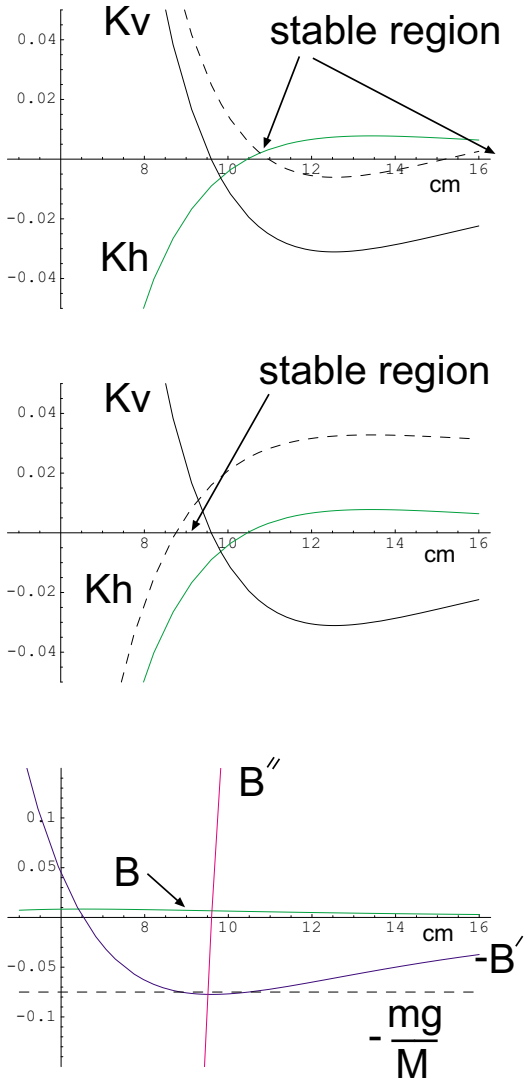

Figure 2: *top:* Stability functions K_v and K_h for a ring lifter magnet with OD 16 cm and ID 10 cm. The x-axis is the distance below the lifter magnet. The dashed line shows the effect of adding diamagnetic plates to stabilize the vertical motion. Levitation is stable where both K_v and K_h are positive. *middle:* The dashed line shows the effect of adding a diamagnetic material to stabilize the radial motion. *bottom:* Magnetic field (T), gradient (T/m), and curvature (T/m^2) of the lifting ring magnet. The dashed line is equal to $-mg/M$ of a NdFeB floater magnet. Where the dashed line intersects the gradient, there will be force balance. If force balance occurs in a stable region, levitation is possible.

The combined conditions for vertically stabilized levitation can be written

$$\frac{2C_z}{M} > B'' > \frac{1}{2B_0}\left(\frac{mg}{M}\right)^2. \tag{15}$$

C_z is proportional to the diamagnetic susceptibility and gets smaller if the gap between the magnet and diamagnet is increased. We can see that the largest gap, or use of weaker diamagnetic material, requires a large B field at the levitation position.

Here it is interesting to note that the inflection point is fixed by the geometry of the lifter magnet, not the strength of the magnet. The instability is related to the curvature of the lifter field and force balance depends on the gradient. That makes it feasible to engineer the location of the stable zones by adjusting the geometry of the lifter magnet and to control the gradient by adjusting the strength. With a solenoid for example, the stable areas will be determined by the radius and length of the solenoid and the current can be adjusted to provide force balance at any location.

The middle plot of figure 2 shows that it is also possible to add a positive C_r to K_h where it turns negative to create a region where both K_v and K_h are positive, just above the inflection point. The bottom plot shows the lifter field, gradient, and curvature on the symmetry axis and the value of $-mg/M$ for a NdFeB floater magnet of the type typically used. (The minus sign is used because the abscissa is in the $-z$ direction. The plotted gradient is the negative of the desired gradient in the $+z$ direction.) Force balance occurs where the dashed line intersects the gradient curve.

5 Evaluating the C_z diamagnetic term

We assume a linear constitutive relation where the magnetization density is related to the applied **H** field by the magnetic susceptibility χ, where χ is negative for a diamagnetic substance.

The magnetic induction **B** inside the material is

$$\mathbf{B} = \mu_0(1+\chi)\mathbf{H} = \mu_0\mu H \tag{16}$$

where μ, the relative magnetic permeability, might be a scalar, vector, or tensor depending on the isotropy properties of the material. A perfect diamagnet such as a Type I superconductor has $\mu = 0$ and will completely cancel

the normal component of an external **B** field at its surface by developing surface currents. A weaker diamagnet will partially expel an external field. The most diamagnetic element in the *Handbook of Chemistry and Physics* is bismuth with $\mu = 0.99983$, just less than the unity of free space. Water, typical of the diamagnetism of living things, has a $\mu = 0.999991$. Even so, this small effect can have dramatic results.

When a magnet approaches a weak diamagnetic sheet of relative permeability $\mu = 1 + \chi \approx 1$ we can solve the problem outside the sheet by considering an image current I' induced in the material but reduced by the factor $(\mu - 1)/(\mu + 1) \approx \chi/2$ (see section 7.23 of Smythe [19]).

$$I' = I\frac{\mu - 1}{\mu + 1} \approx I\frac{\chi}{2}. \tag{17}$$

If the material were instead a perfect diamagnet such as a superconductor with $\chi = -1$ and $\mu = 0$, an equal and opposite image is created as expected.

To take the finite size of the magnet into account we should treat the magnet and image as ribbon currents but first, for simplicity, we will use a dipole approximation which is valid away from the plates and in some other conditions to be described. The geometry is shown in figure 3.

5.1 Dipole approximation of C_z

We will find the force on the magnet dipole by treating it as a current loop subject to $\boldsymbol{I} \times \boldsymbol{B}$ force from the magnetic field of the image dipole. The image dipole is inside a diamagnetic slab a distance D

$$D = 2d + L \tag{18}$$

from the center of a magnet in free space and has strength determined by equation 17. The magnet has length L and radius R and is positioned at the origin of a coordinate system at $z = 0$. We only need the radial component of the field from the induced dipole, B_{ir} at $z = 0$.

Using the field expansion equations 7 and 9 for the case of the image dipole we have

$$B_{ir} = -\frac{1}{2}B_i' r = \frac{\mu_0 \chi M}{8\pi}\frac{3r}{D^4}. \tag{19}$$

The lifting force is

$$F_i = I 2\pi R B_{ir} = \frac{M 2\pi R}{\pi R^2} B_{ir} = \frac{3M^2|\chi|\mu_0}{4\pi D^4}. \tag{20}$$

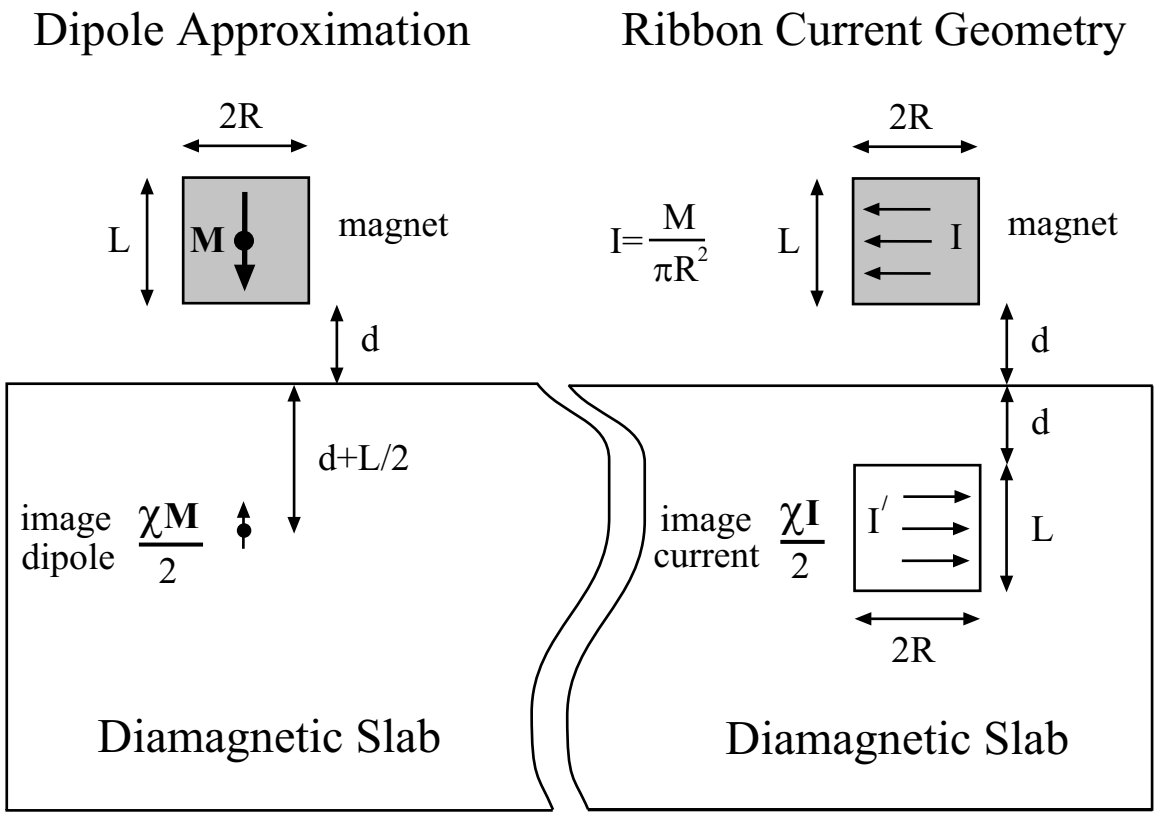

Figure 3: Geometry for the image dipole and image ribbon current force calculations.

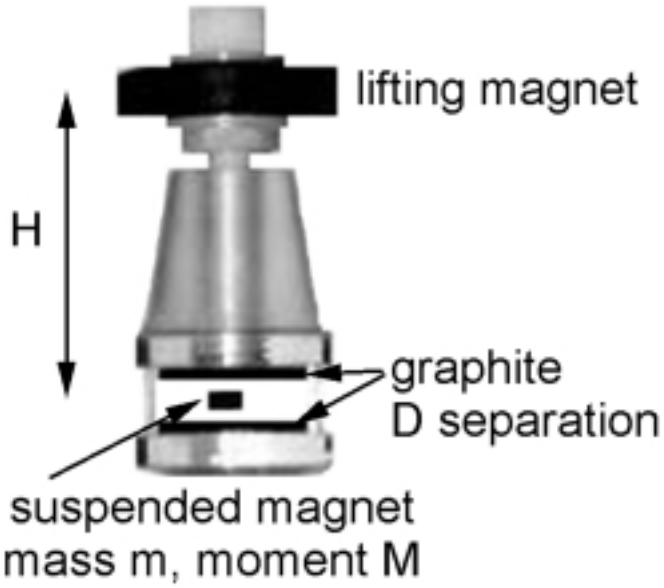

Figure 4: Diamagnetically stabilized magnet levitation geometry for one compact implementation.

For equilibrium at $z = 0$, the lifting force will be balanced by the lifting magnet and gravity so that the net force is zero. The net force from two diamagnetic slabs will also be zero if the magnet is centered between the two slabs as shown in figure 4. This is the case we want to consider first.

We now find the restoring force for small displacements in the z-direction from one slab on the bottom.

$$\frac{\partial F_i}{\partial d} z = \frac{\partial F_i}{\partial D} 2z = -\frac{6M^2|\chi|\mu_0}{\pi D^5} z \tag{21}$$

For the case of a magnet centered between two slabs of diamagnetic material, the restoring force is doubled. We can equate this restoring force to the $C_z z^2$ term in the energy expansion equation 11. We take the negative gradient of the energy term to find the force in the z-direction and equate the terms. For the two slab case

$$\begin{aligned} -2C_z z &= -2\frac{6M^2|\chi|\mu_0}{\pi D^5} z \\ C_z &= \frac{6M^2|\chi|\mu_0}{\pi D^5} \end{aligned} \tag{22}$$

5.2 Alternate route to C_z

The same result can be derived directly from the equation for the potential energy of a magnet with fixed dipole M in the induced field B_i of its image in a para or diamagnetic material [19]

$$U_i = -\frac{1}{2}\mathbf{M}\cdot\mathbf{B_i}. \tag{23}$$

We assume that the magnet is in equilibrium with gravity at $z = 0$ due to forces from the lifter magnet and possibly forces from the diamagnetic material and we want to calculate any restoring forces from the diamagnetic material. The energy of the floater dipole M in the fields B_i of the induced dipoles from diamagnetic slabs above and below the magnet is

$$U_i = \frac{|\chi|M^2\mu_0}{8\pi}\left[\frac{1}{(2d+l+2z)^3}+\frac{1}{(2d+l-2z)^3}\right] \tag{24}$$

We expand the energy around the levitation point $z = 0$

$$\begin{aligned} U_i &= U_{i0} + U_i' z + \frac{1}{2}U_i'' z^2 + \ldots & (25)\\ &= \frac{|\chi|M^2\mu_0}{8\pi}\left[\frac{2}{(2d+l)^3}+\frac{48}{(2d+l)^5}z^2\right]+\ldots & (26)\\ &= C + \frac{6|\chi|M^2\mu_0}{\pi D^5}z^2+\ldots & (27)\\ &= C + C_z z^2 + \ldots. & (28)\end{aligned}$$

This gives the same result as equation 22.

5.3 Maximum gap D in dipole approximation

Adding diamagnetic plates above and below the floating magnet with a separation D gives an effective energy due to the two diamagnetic plates

$$U_{dia} \equiv C_z z^2 = \frac{6\mu_0 M^2|\chi|}{\pi D^5}z^2 \tag{29}$$

in the dipole approximation. From the stability conditions (eq. 13,14), we see that levitation can be stabilized at the point where $B' = mg/M$ if

$$\frac{12\mu_0 M|\chi|}{\pi D^5} > B'' > \frac{(mg)^2}{2M^2 B_0} \tag{30}$$

This puts a limit on the diamagnetic gap spacing

$$D < \left\{ \frac{12\mu_0 M|\chi|}{\pi B''} \right\}^{\frac{1}{5}} < \left\{ \frac{24\mu_0 B_0 M^3|\chi|}{\pi(mg)^2} \right\}^{\frac{1}{5}} \tag{31}$$

If we are far from the lifter magnet field, we can consider it a dipole moment M_L at a distance H from the floater. The equilibrium condition, equation 12, is

$$H = \left\{ \frac{3MM_L\mu_0}{2\pi mg} \right\}^{\frac{1}{4}} \tag{32}$$

Then, the condition for stability and gap spacing at the levitation point is [20]

$$D < H\left\{ 2|\chi|\frac{M}{M_L} \right\}^{\frac{1}{5}} \tag{33}$$

The most important factor for increasing the gap is using a floater with the strongest possible M/m. Using the strongest diamagnetic material is also important. Lastly, a stronger lifting dipole further away (larger H) produces some benefit.

5.4 Surface current approximation

Treating the magnets and images as dipoles is useful for understanding the general dependencies but if the floater magnet is large compared to the distance to the diamagnetic plates, there will be significant errors. These errors can be seen in equation 29 where the energy becomes infinite as the distance $D = 2d + L$ goes to zero. Since the gap spacing d is usually on the order of the floater magnet radius and thickness, more accurate calculations of the interaction energy are necessary. (In the special case when the diameter of a cylindrical magnet is about the same as the magnet length, the dipole approximation is quite good over the typical distances used as can be confirmed in figure 6.)

Even treating the lifter magnet as a dipole is not a very good approximation in most cases. A better approximation for the field B_L from a simple cylindrical lifter magnet of length l_L and radius R_L at a distance H from the bottom of the magnet is

$$B_L = \frac{B_{Lr}}{2}\left[\frac{H + l_L}{\sqrt{(H + l_L)^2 + R_L^2}} - \frac{H}{\sqrt{H^2 + R_L^2}} \right] \tag{34}$$

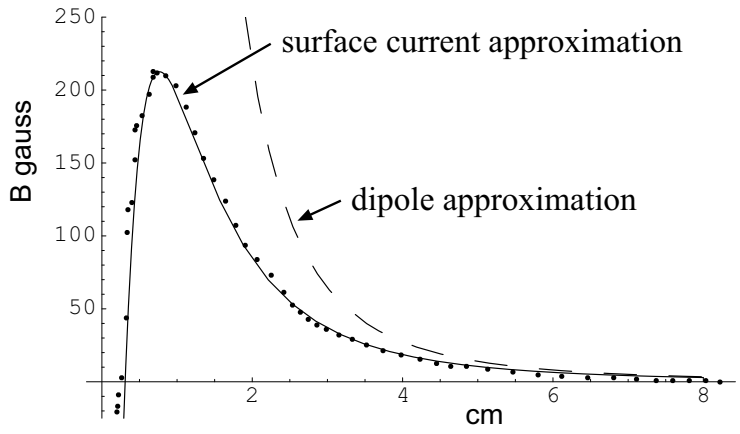

Figure 5: Measured field from a ring lifter magnet with fits to a dipole approximation and a surface current approximation. The lifter is a ceramic material with B_r of 3,200 gauss. The dimensions are O.D. 2.8 cm, I.D. 0.9 cm, and thickness 0.61 cm.

where B_{Lr} is the remanent or residual flux density of the permanent magnet material. (The residual flux density is the value of B on the demagnetization B-H curve where H is zero when a closed circuit of the material has been magnetized to saturation. It is a material property independent of the size or shape of the magnet being considered.) This equation is equivalent to using a surface current or solenoid model for the lifter magnet and is a very good approximation. If the lifter is a solenoid B_{Lr} is the infinite solenoid field $\mu_0 NI/l_L$.

Figure 5 shows the measured field of a lifter ring magnet we used. The fit of the surface current approximation is better even 4 cm away which was approximately the levitation force balance position. The ring magnet has an additional equal but opposite surface current at the inner diameter which can be represented by a second equation of form 34.

6 Method of image currents for evaluating C_z

The force between two parallel current loops of equal radii a separated by a distance c with currents I and I' can be written as (see section 7.19 of

Smythe [19])

$$F_{loops} = \mu_0 II' \frac{c}{\sqrt{4a^2 + c^2}} \left[-K + \frac{2a^2 + c^2}{c^2} E \right] \tag{35}$$

where K and E are the elliptic integrals

$$K = \int_0^{\frac{\pi}{2}} \frac{1}{\sqrt{1 - k^2 \sin^2 \theta}} \, d\theta \tag{36}$$

$$E = \int_0^{\frac{\pi}{2}} \sqrt{1 - k^2 \sin^2 \theta} \, d\theta \tag{37}$$

and

$$k^2 = \frac{4a^2}{4a^2 + c^2} \tag{38}$$

We extend this analysis to the case of two ribbon currents because we want to represent a cylindrical permanent magnet and its image as ribbon currents. The geometry is shown in figure 3. We do a double integral of the loop force equation 35 over the length dimension L of both ribbon currents. With a suitable change of variables we arrive at the single integral

$$F = \mu_0 II' \int_{-1}^{1} J\{1 - v sgn(v)\} dv \tag{39}$$

where

$$\begin{aligned} J &= \sqrt{1 - k^2} \left[\frac{1 - \frac{1}{2}k^2}{1 - k^2} E(k) - K(k) \right] && (40) \\ k &= \frac{1}{\sqrt{1 + \gamma^2}} \\ \gamma &= \frac{d}{R} + \frac{L}{2R}(1 + v) \\ sgn(v) &= \text{sign of } v \\ &= \begin{cases} +1 & if \quad v > 0 \\ 0 & if \quad v = 0 \\ -1 & if \quad v < 0 \end{cases} && (41) \end{aligned}$$

d is the distance from the magnet face to the diamagnetic surface and R and L are the radius and length of the floating magnet.

From measurements of the dipole moment M of a magnet, we convert to a current

$$I = \frac{M}{\text{area}} = \frac{M}{\pi R^2}. \tag{42}$$

Using equation 17, we have

$$I' = \frac{\chi M}{2\pi R^2}. \tag{43}$$

Once M, χ, and the magnet dimensions are known, equation 39 can be integrated numerically to find the force. If the force is measured, this equation can be used to determine the susceptibility χ of materials. We used this method to make our own susceptibility measurements and this is described below.

In the vertically stabilized levitation configuration shown in figure 4, there are diamagnetic plates above and below the floating magnet and at the equilibrium point, the forces balance to zero. The centering force due to the two plates is twice the gradient of the force F in equation 39 with respect to d, the separation from the diamagnetic plate, times the vertical displacement z of the magnet from the equilibrium position. We can equate this force to the negative gradient of the $C_z z^2$ energy term from equation 11

$$-2C_z z = 2\frac{\partial F}{\partial d} z. \tag{44}$$

Therefore, the coefficient C_z in equations 11 and 13 is

$$C_z = -\frac{\partial F}{\partial d} \tag{45}$$

and this force must overcome the instability due to the unfavorable field curvature B''. Figure 6 shows the force and gradient of the force for floating magnets of different aspect ratios.

6.1 Oscillation frequency

When the vertical stability conditions (equation 13) are met, there is an approximately quadratic vertical potential well with vertical oscillation frequency

$$\nu = \frac{1}{2\pi}\sqrt{\frac{1}{m}\left\{-2\frac{\partial F}{\partial d} - MB''\right\}} \tag{46}$$

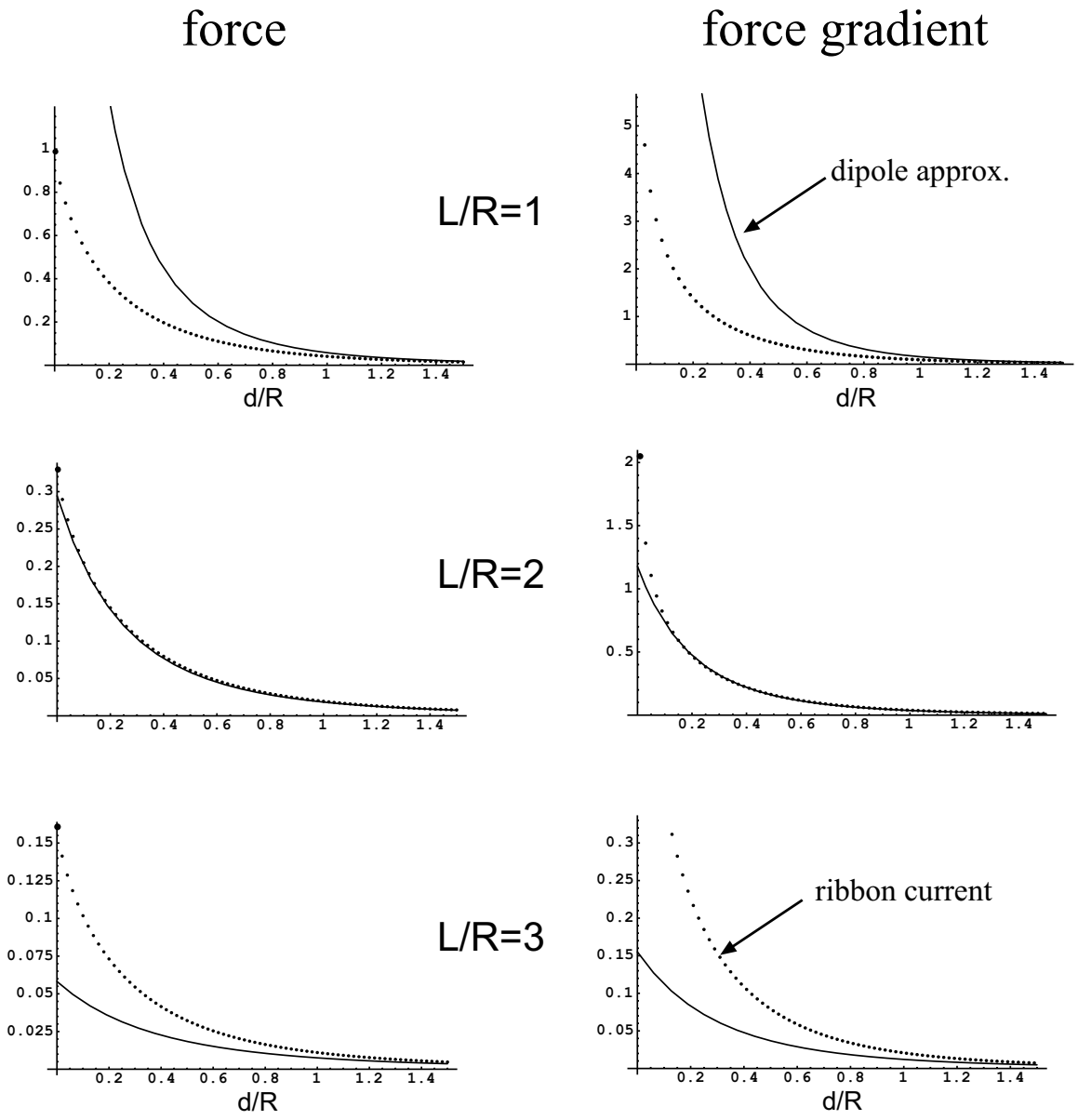

Figure 6: Dipole approximation compared to image current solution for three different magnet length to radius ratios. The force axis is in units of $\mu_0 I^2 \chi/2$. The ribbon current I is related to the dipole moment M of the magnet by $M = I\pi R^2$. The force gradient axis is in units $-\mu_0 I^2 \chi/2R$.

Applying equation 22, in the dipole approximation, the vertical bounce frequency is

$$\nu = \frac{1}{2\pi}\sqrt{\frac{1}{m}\left\{\frac{12\mu_0 M^2|\chi|}{\pi D^5} - MB''\right\}}. \tag{47}$$

The expressions in the curly braces, $2K_v$, represents the vertical stiffness of the trap. $2K_h$ represents the horizontal stiffness.

The theoretical and measured oscillation frequencies are shown later in figure 12. It is seen that the dipole approximation is not a very good fit to the data whereas the image current prediction is an excellent fit.

7 The C_r term

We now consider the case just above the inflection point where $B'' < 0$. A hollow diamagnetic cylinder with inner diameter D as shown in figure 7 produces an added energy term (in the dipole approximation) [3]

$$U_{dia} \equiv C_r r^2 = \frac{45\mu_0|\chi|M^2}{16D^5} r^2 \tag{48}$$

Near the inflection point where B'' is negligible, the horizontal stability condition equation 14 becomes

$$\frac{45\mu_0|\chi|M^2}{2D^5} > \frac{MB'^2}{B_0} = \frac{m^2 g^2}{MB_0} \tag{49}$$

$$D < \left\{\frac{45\mu_0 B_0 M^3|\chi|}{2(mg)^2}\right\}^{\frac{1}{5}} \tag{50}$$

This type of levitator can also be implemented on a tabletop using a large diameter permanent magnet ring as a lifter as described in the middle plot of figure 2.

The horizontal bounce frequency in the approximately quadratic potential well is

$$\nu_r = \frac{1}{2\pi}\sqrt{\frac{1}{m}\left\{\frac{45\mu_0 M^2|\chi|}{8D^5} + \frac{MB''}{2} - \frac{MB'^2}{4B_0}\right\}}. \tag{51}$$

The expression in the curly braces, $2K_h$, represents the horizontal stiffness of the trap.

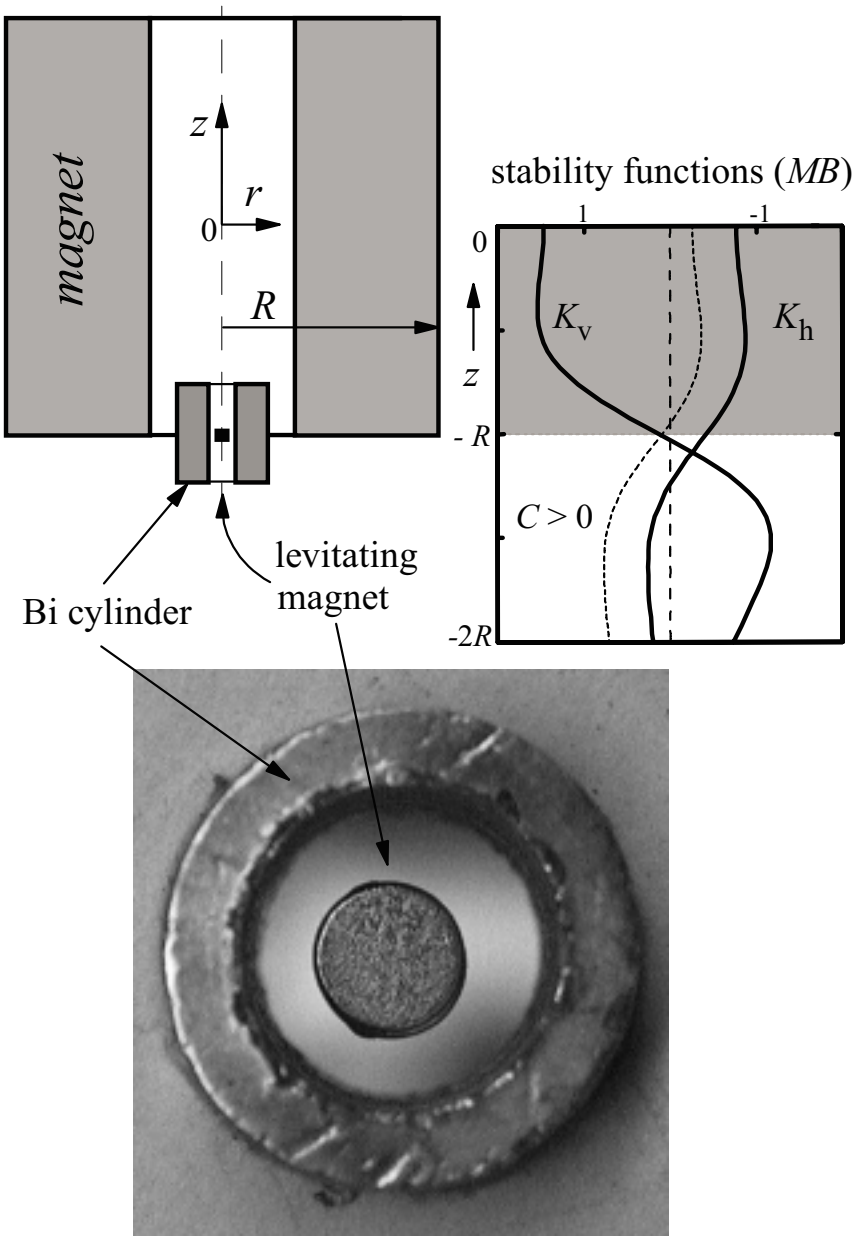

Figure 7: Vertical and horizontal stability curves for magnet levitation showing the stabilizing effect of a diamagnetic cylinder with an inner diameter of 8 mm and the levitation geometry. Magnet levitation is stable where both curves are positive and the magnetic lifting force matches the weight of the magnet.

8 Counterintuitive levitation configuration

There is another remarkable but slightly counterintuitive stable levitation position. It is above a lifter ring magnet with the floater in an attractive orientation. Even though it is in attractive orientation, it is vertically stable and horizontally unstable. The gradient from the lifter repels the attracting magnet but the field doesn't exert a flipping torque. This configuration is a reminder that it is not the field direction but the field gradient that determines whether a magnet will be attracted or repelled. A bismuth or graphite cylinder can be used to stabilize the horizontal instability.

Figure 8 shows the stability functions and magnetic fields for this levitation position above the lifter magnet. We have confirmed this position experimentally.

9 Experimental results

Before we can compare the experimental results to the theory, we need to know the values of the magnetic dipole moment of the magnets and the susceptibility of diamagnetic materials we use. The dipole moment can be determined by measuring the $1/r^3$ fall of the magnetic field on axis far from a small magnet. For $Nd_2Fe_{14}B$ magnet material, it is an excellent approximation to consider the field as created by a solenoidal surface current and use the finite solenoid equation (34) fit to measurements.

The diamagnetic susceptibility was harder to measure. Values in the *Handbook of Chemistry and Physics* were problematic. Most sources agree on some key values such as water and bismuth. (There are multiple quantities called susceptibility and one must be careful in comparing values. Physicists use what is sometimes referred to as the volume susceptibility. Chemists use the volume susceptibility divided by the density. There is also a quantity sometimes called the gram molecular susceptibility which is the volume susceptibility divided by the density and multiplied by the molecular weight of the material. There are also factors of 4π floating around these definitions. In this paper we use the dimensionless volume susceptibility in SI units).

The values given in the *Handbook of Chemistry and Physics* and other some other published sources for graphite are inexplicably low. This could be because graphite rods have many different compositions and impurities. Iron is a major impurity in graphite and can overwhelm any diamagnetic

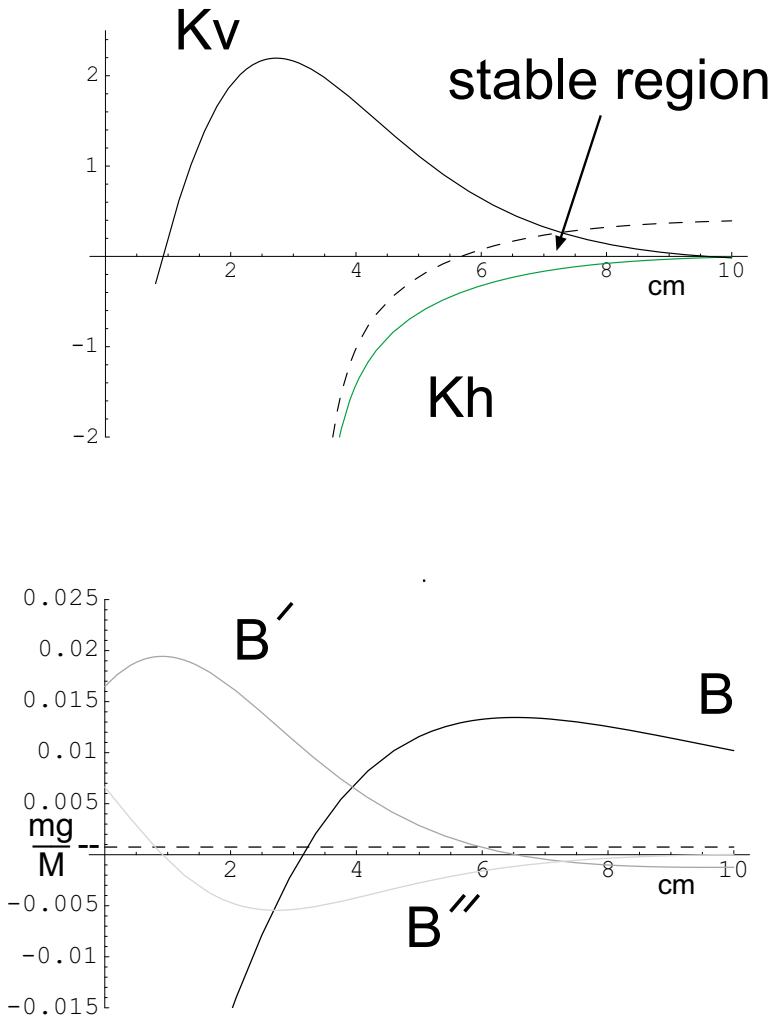

Figure 8: *top:* Vertical and horizontal stability curves for magnet levitation a distance H above a ring lifter magnet. The dashed line shows the stabilizing effect of a diamagnetic cylinder. Magnet levitation is stable where both curves are positive and the magnetic lifting force matches the weight of the magnet. *bottom:* B (T), B' (T/cm), B'' (T/cm^2), and mg/M (T/cm) for a 16 cm OD, 10 cm ID, 3 cm thick ring lifting magnet and a NdFeB floater.

effect. We have seen graphite rods that are diamagnetic on one end and paramagnetic on the other. Braunbek noticed that used graphite arc rods were more diamagnetic on the side closest the arc. He speculated that the binder used in the rods was paramagnetic and was vaporized by the heat of the arc. We found that in practice, purified graphite worked as well as bismuth and our measurements of its susceptibility were consistent with this.

Values for a form of graphite manufactured in a special way from the vapor state called pyrolytic graphite, are not given in the *Handbook* and the other literature gives a wide range of values. Pyrolytic graphite is the most diamagnetic solid substance known. It has an anisotropic susceptibility. Perpendicular to the planar layers, the diamagnetic susceptibility is better than in pure crystal graphite [21]. Parallel to the planar layers, the susceptibility is lower than randomly oriented pressed graphite powder.

We developed a technique to measure the diamagnetic susceptibility of the materials we used. Later, we were able to get a collaborator (Fred Jeffers) with access to a state of the art vibrating sample magnetometer to measure some samples. There was very good agreement between our measurements and those made using the magnetometer.

9.1 Measurements of diamagnetic susceptibility

A simple and useful method for testing whether samples of graphite are diamagnetic or not (many have impurities that destroy the diamagnetism) is to hang a small NdFeB magnet, say 6 mm diameter as the bob of a pendulum with about 1/2 m of thread. A diamagnetic graphite piece slowly pushed against the magnet will displace the pendulum a few cm before it touches, giving a quick qualitative indication of the diamagnetism.

The method we used to accurately measure the susceptibility was to hang a small NdFeB magnet as a pendulum from pairs of long threads so that the magnet could move along only one direction. The magnet was attached to one end of a short horizontal drinking straw. At the other end of the straw, a small disk of aluminum was glued. A translation stage was first zeroed with respect to the hanging magnet without the diamagnetic material present. Then the diamagnetic material to be tested was attached to a micrometer translation stage and moved close to magnet, displacing the pendulum from the vertical. The force was determined by the displacement from vertical of the magnet and χ was determined from equations 39 and 17 which is plotted as the force in figure 6.

A sample of bismuth was used as a control and matched the value in the standard references [22]. Once the value for our sample of bismuth was confirmed, the displacement was measured for a fixed separation d between the magnet and bismuth. All other samples were then easily measured by using that same separation d; the relative force/translation giving the susceptibility relative to bismuth.

The difficult part was establishing a close fixed distance between the magnet and the diamagnetic material surface with high accuracy. This problem was solved by making the gap part of a sensitive LC resonant circuit. Attached to the translation stage a fixed distance from the diamagnetic material under test, was the L part of the LC oscillator. When the gap between the diamagnet and magnet reached the desired fixed value, the flat piece of aluminum on the other side of the straw from the magnet, came a fixed distance from the L coil, changing its inductance. The separation distance could be set by turning a micrometer screw to move the translation stage until the frequency of the LC circuit reached the predetermined value for each sample under test. The setup is shown in figure 9.

This method was perhaps more accurate for our purposes than the vibrating sample magnetometer, an expensive instrument. Our method was independent of the volume of the diamagnetic material. The vibrating sample magnetometer is only as accurate as the volume of the sample is known. Samples are compared to a reference sample of nickel with a specific geometry. Our samples were not the same geometry and there was some uncertainty in the volume. Our measurements measured the susceptibility of the material in a way relevant to the way the material was being used in our experiments.

We measured various samples of regular graphite and pyrolytic graphite and bismuth. Our average values for the graphite materials are shown in table 1 and are consistent with the values from the vibrating sample magnetometer. Our value for graphite is higher than many older values such as that reported in the *Handbook of Chemistry and Physics*, but is lower than that stated in a more recent reference [23]. Our values for pyrolytic graphite are below the low end of the values stated in the literature [18, 24]. The value for the pyrolytic graphite parallel to the planar layers is from the vibrating sample magnetometer.

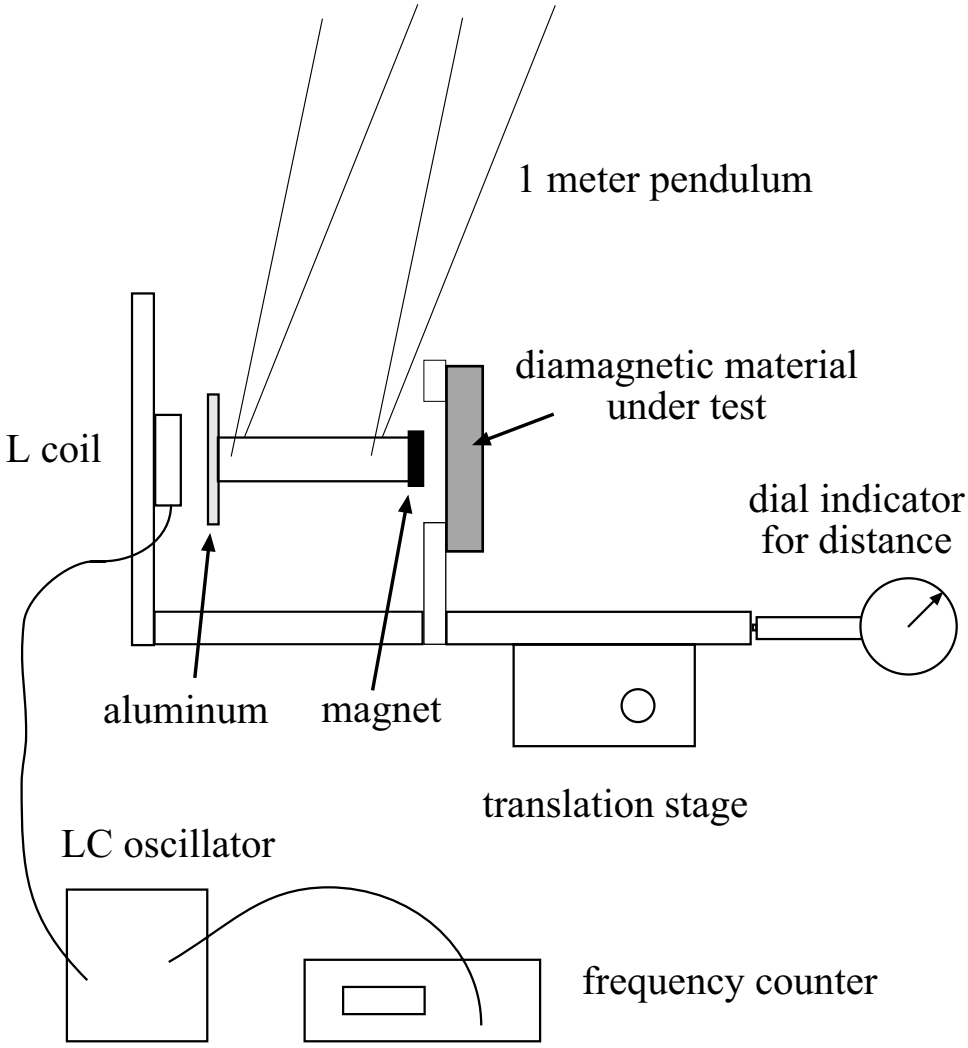

Figure 9: Setup for measuring diamagnetic susceptibility. The diamagnetic material is moved close to the magnet, deflecting the magnet pendulum, until the gap between the magnet and diamagnet reaches a preset value. When the aluminum is a fixed distance from the inductor coil, the LC circuit resonates at the desired frequency, corresponding to the preset value of the gap. This is an accurate way to measure the small gap. The force is determined from the displacement of the pendulum. The force is then compared to the force from a previously calibrated sample of bismuth with the same gap.

9.2 Experimental realization of levitation

The fingertip and book stabilized levitation shown in figure 1 was achieved using a 1 m diameter 11 T superconducting solenoid 2.5 m above the levitated magnet where the field was 500 G. Using regular graphite and an inexpensive ceramic lifter magnet it is possible to make a very stable levitator about 5 cm tall with a gap D of about 4.4 mm for a 3.175 mm thick 6.35 mm diameter NdFeB magnet. Using pyrolytic graphite, the gap D increases to almost 6 mm for the same magnet. This simple design (similar to figure 4) could find wide application. The stability curves and gradient matching condition can be seen in figure 10. The magnitude of C_z was determined from the force gradient of figure 6 with $L/R = 1$ at two different gaps d using our measured susceptibility of pyrolytic graphite.

Figure 7 shows an experimental realization of horizontal stabilization at the High Field Magnet Laboratory in Nijmegen. We also achieved horizontal stabilization on a tabletop using a permanent magnet ring and a graphite cylinder.

We were recently able to achieve stable levitation at the counterintuitive position above the ring lifter magnet (described above). The floater is in attractive orientation but is naturally vertically stable and radially unstable. Radial stabilization was provided by a hollow graphite cylinder.

Other configurations for diamagnetically stabilized magnet levitation are possible and rotational symmetry is not required. For example, at the levitation position described just above, if an oval magnet or a noncircular array is used for a lifter instead of a circular magnet, the $x - z$ plane can be made stable. Instead of using a hollow cylinder to stabilize the horizontal motion, flat plates can be used to stabilize the y direction motion.

For vertical stabilization with flat plates, if a long bar magnet is used horizontally as a lifter, the levitation point can be turned into a line. With a ring magnet, the equilibrium point can be changed to a circle. Both of these tricks have been demonstrated experimentally.

Another quite different configuration is between two vertical magnet pole faces as shown in figure 11. Between the pole faces, below center and just above the inflection point in the magnetic field magnitude, the floating magnet is naturally vertically stable. Diamagnetic plates then stabilize the horizontal motion. To our knowledge, this configuration was first demonstrated by S. Shtrikman.

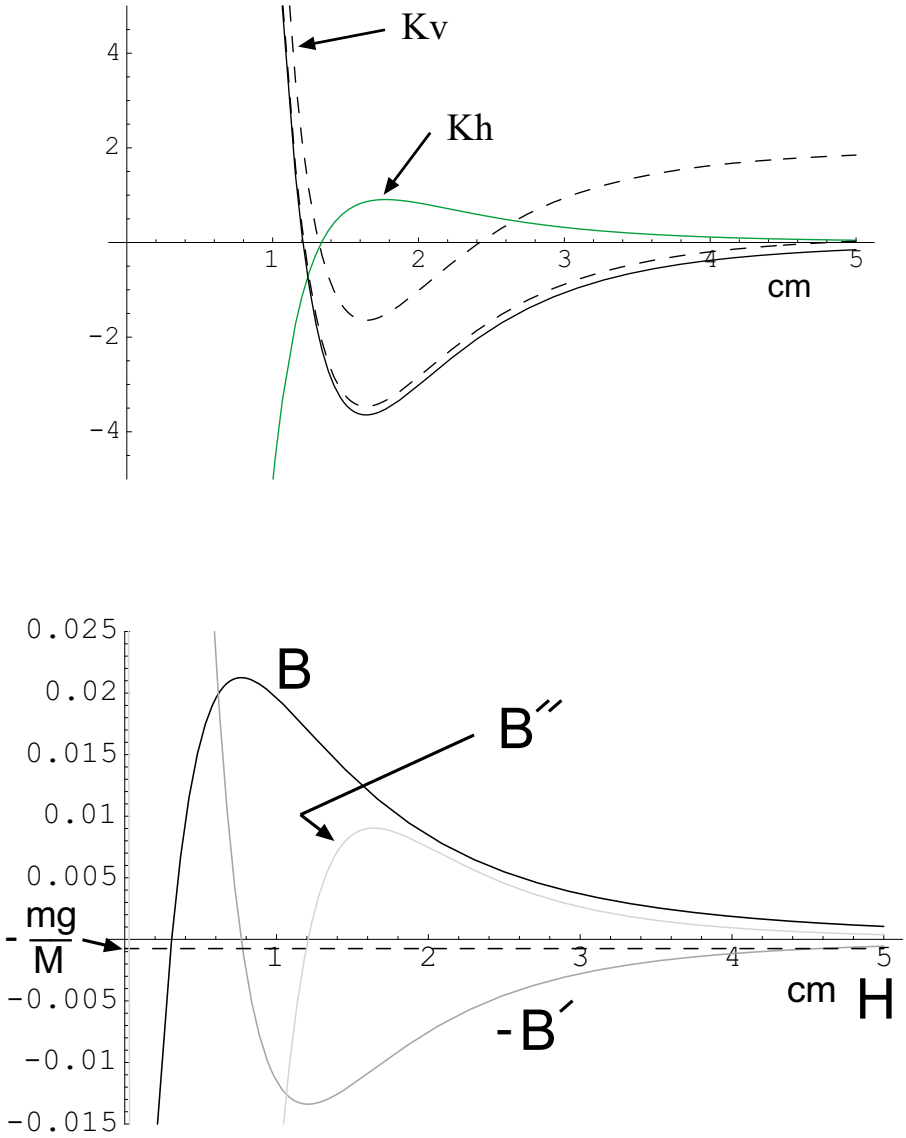

Figure 10: *top:* Stability functions K_v and K_h for the demonstration levitator. Stability is possible where both functions are positive. The dashed lines show the effect of two different values of the C_z term on K_v. The smaller value corresponds to a large gap spacing $d = 1.9$ mm. The larger value corresponds to a gap of only 0.16 mm. *bottom:* The levitation position is where $-mg/M$ intersects the gradient $-B'$ at approximately $H = 4.5$ cm below the lifter magnet. B in T, $-B'$ in T/cm, and B'' in T/cm^2.

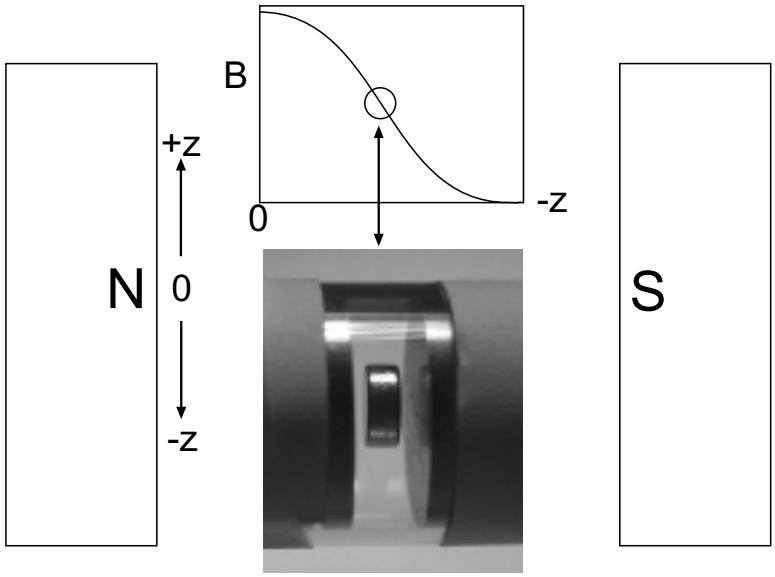

Figure 11: Graphite plates stabilize levitation of a magnet below the centerline between two pole faces and just above the inflection point in the field magnitude. Not shown in the picture but labelled N and S in the figure are the 25 cm diameter pole faces of an electromagnet spaced about 15 cm apart. The poles can be from permanent or electromagnets.

9.3 Measurements of forces and oscillation frequencies

One way to probe the restoring forces of the diamagnetic levitator is to measure the oscillation frequency in the potential well. For the vertically stabilized levitator of figure 4 we measured the vertical oscillation frequency as a function of the gap spacing d and compared it to the dipole and image current forces and prediction equations 46 and 47. The lifting magnet used for this experiment was a 10 cm long by 2.5 cm diameter cylindrical magnet. This magnet was used because its field could be accurately determined from the finite solenoid equation. The dipole moment was measured to be 25 Am^2. The floater magnet was a 4.7 mm diameter by 1.6 mm thick NdFeB magnet with a dipole moment of 0.024 Am^2. It weighed 0.22 grams and levitated 8 cm below the bottom of the lifter magnet as expected.

The graphite used was from a graphite rod, not pyrolytic graphite. We measured this sample of graphite to have a susceptibility of -170×10^{-6}. The oscillation frequency was determined by driving an 1800 Ohm coil below the levitated magnet with a sine wave. The resonant frequency was determined visually and the vibration amplitude kept small. The gap was changed by carefully turning a $\frac{1}{4}$–20 screw.

Figure 12 shows the theoretical predictions and the experimental measurements of the oscillation frequency as a function of gap spacing d. There are no adjustable parameters in the theory predictions. All quantities were measured in independent experiments. The agreement between the data and the image current calculation is remarkably good. There is a limit to how much the total gap $D = 2d + l$ can be increased. If D is too great, the potential well becomes double humped and the magnet will end up closer to one plate than the other. The last point with d greater than 1.4 mm was clearly in the double well region and was plotted as zero.

10 Levitation solutions for a cylindrically symmetric ring magnet

A ring magnet provides many combinations of fields, gradients and curvatures as shown in figure 13. Considering the field topology but not the magnitudes, we show all possible positions where diamagnets, spin-stabilized magnets, and magnets stabilized by diamagnetic material can levitate. The fields and gradients shown may not be sufficient to levitate a diamagnet in the position

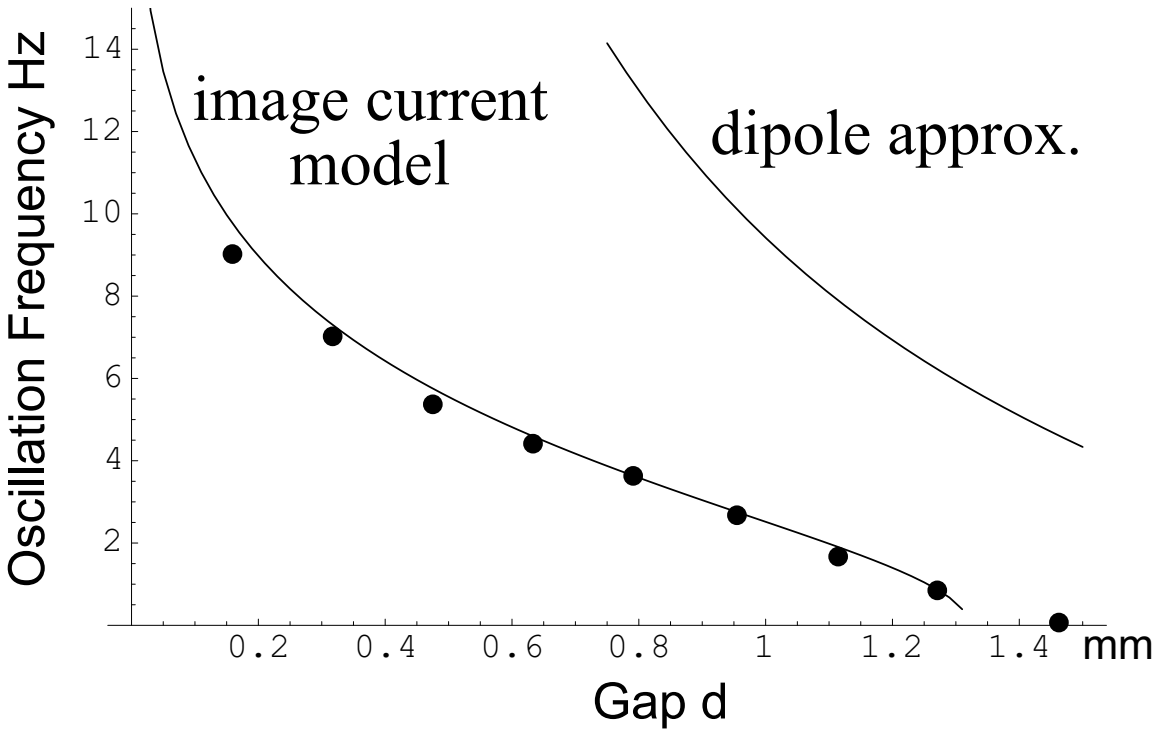

Figure 12: Data points on the vertical oscillation frequency versus the gap spacing d with the dipole approximation prediction curve and the image current theory curve. The curves are not fit to the data. They are predictions from the measured properties of the magnets and diamagnets, with no free parameters. The last point is beyond the zero frequency limit and is plotted as zero. At zero frequency, the gap is too large to provide stability and the potential well becomes double humped, with stable points closer to one plate than the other. This clearly was the case with the last point around $d > 1.4$ mm.

Table 2: Magnetic field requirements for levitation of diamagnets, spin-stabilized magnet levitation, and diamagnetically stabilized levitation of magnets. + and – indicate the sign with respect to the sign of B.

	M aligned with B	B'	B''
levit. of diamagnets	–	–	+ or –
spin-stabilized magnet	–	–	+
diamag. stab. horiz.	+	+	–
diamag. stab. vert.	+	+	+

Table 3: Stability functions for levitation of diamagnets, spin-stabilized magnets, and diamagnetically stabilized magnets. The functions must be positive for stability and assume B_0 in the positive z direction.

	vertical	horizontal
levit. of diamagnets	$B_0 B'' + B'^2$	$B'^2 - 2B_0 B''$
spin-stabilized magnet	B''	$B'^2 - 2B_0 B''$
diamag. stab. magnet	$C_z - \frac{1}{2} M B''$	$C_r + \frac{1}{4} M \left\{ B'' - \frac{B'^2}{2B_0} \right\}$

shown against 1 g of gravity, but the topology is correct if the magnetic field could be increased enough.

Each type of levitation has its own requirements for radial and horizontal stability and the stable regions for each are shown. Other requirements such as matching the magnetic field gradient to mg/M need be met. The fields must be in the right direction so as not to flip the magnet. These required directions of B, B', and B'' are shown in table 2. The directions are all compared to the direction of B.

The most fruitful place to look for levitation positions is around the inflection points of the magnetic field. These are the places where the instability is weakest. The two levitation regions in figure 13 marked with a question mark have not been demonstrated experimentally and are probably not accessible with current magnetic and diamagnetic materials. The lower position with a question mark would work using a diamagnetic cylinder for radial stabilization. However, it may require more diamagnetism than is available. The levitation positions without the question marks have been demonstrated experimentally. The position for levitation of a diamagnet marked with the * has been recently demonstrated by the authors.

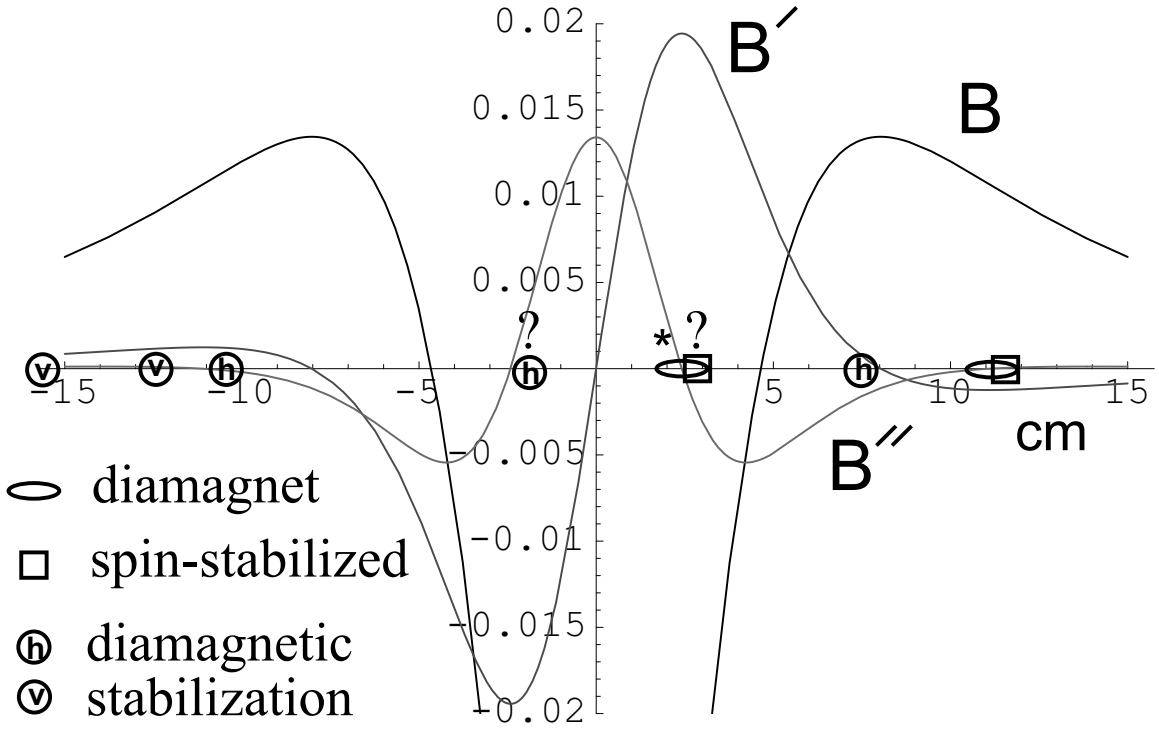

Figure 13: B (T), B' (T/cm), and B'' (T/cm^2), for a 16 cm OD, 10 cm ID, 3 cm thick ring lifting magnet showing the fields on axis above and below the magnet. All possible levitation positions are shown for spin-stabilized magnet levitation, diamagnetically stabilized magnet levitation, and levitation of diamagnets. h and v indicate use of diamagnetic material for horizontal or vertical stabilization. The two regions with question marks have not yet been verified experimentally and may be difficult to achieve. The levitation of diamagnets marked with * has recently been demonstrated by the authors.

The locations for diamagnetically stabilized magnet levitation are interesting for another reason. At these locations servo control can be used to provide active stabilization very efficiently, since the instability is weak at those locations. The diamagnetic plates or cylinder act as a very weak servo system.

Acknowledgements

We acknowledge fruitful communications with Michael Berry. We would like to thank Marvin Drandell for his help fabricating many prototype levitators, Rudy Suchannek for his translation of Braunbek's [10] papers from German, and Fred Jeffers for helping confirm our susceptibility measurements.

References

[1] M. V. Berry and A. K. Geim, "Of flying frogs and levitrons", *Euro. J. Phys.*, **18**, 307–313 (1997) and http://www-hfml.sci.kun.nl/hfml/levitate.html.

[2] A. Geim, "Everyone's Magnetism", *Phys. Today*, **51** Sept., 36–39 (1998).

[3] A. K. Geim, M. D. Simon, M. I. Boamfa, L. O. Heflinger, "Magnet levitation at your fingertips", *Nature*, **400**, 323–324 (1999).

[4] M. D. Simon and A. K. Geim, "Diamagnetic levitation; Flying frogs and floating magnets", *J. App. Phys.*, **87**, 6200–6204 (2000).

[5] N. W. Ashcroft and N. D. Mermin, *Solid State Physics*, ch. 31, 647, Harcourt Brace, New York, (1976).

[6] R. P. Feynman, R. B. Leighton, and M. Sands, *The Feynman Lectures in Physics, vol. II*, chp. 34 sec. 6, Addison-Wesley Publishing Company, New York (1963).

[7] S. Earnshaw, "On the nature of the molecular forces which regulate the constitution of the luminiferous ether", *Trans. Camb. Phil. Soc.*, **7**, 97-112 (1842).

[8] K. T. McDonald, "Laser tweezers", *Am. J. Phys.*, **68**, 486–488 (2000).

[9] W. Thomson, "Reprint of Papers on electrostatics and magnetism", XXXIII, 493-499, and XXXIV, 514-515, London, MacMillan (1872).

[10] W. Braunbek, "Freischwebende Körper im elecktrischen und magnetischen Feld" and "Freies Schweben diamagnetischer Körper im Magnetfeld" *Z. Phys.*, **112**, 753–763 and 764–769 (1939).

[11] V. Arkadiev, "A floating magnet", *Nature*, **160**, 330 (1947).

[12] R. M. Harrigan, U.S. patent 4,382,245, (1983).

[13] M. D. Simon, L. O. Heflinger, and S. L. Ridgway, "Spin stabilized magnetic levitation", *Am. J. Phys.*, **65**, 286–292 (1997).

[14] M. V. Berry, "The Levitron^{TM}: an adiabatic trap for spins", *Proc. Roy. Soc. Lond. A*, **452**, 1207–1220 (1996).

[15] Personal communication with Ed Phillips.

[16] V. V. Vladimirskii, "Magnetic mirrors, channels and bottles for cold neutrons", *Sov. Phys. JETP*,**12**,740-746 (1961) and W. Paul, "Electromagnetic traps for charged and neutral particles", *Rev. Mod. Phys.*, **62**, 531-540 (1990).

[17] A. H. Boerdijk, "Technical aspects of levitation", *Philips Res. Rep.*, **11**, 45–56 (1956) and A. H. Boerdijk, "Levitation by static magnetic fields", *Philips Tech. Rev.*, **18**, 125–127 (1956/57).

[18] V. M. Ponizovskii, "Diamagnetic suspension and its applications (survey)", *Prib. Tek. Eksper.*, **4**, 7–14 (1981).

[19] W. R. Smythe, *Static and Dynamic Electricity*, Hemisphere Publishing Corporation, New York, third ed., (1989).

[20] M. V. Berry first suggested the simplification of treating the lifter magnet as a dipole and derived equation 33 in a 1997 correspondence with M. D. Simon.

[21] D. B. Fischback, "The magnetic susceptibility of pyrolytic carbons", *Proceedings of the Fifth Conference on Carbon*, **2**, 27–36,(1963).

[22] For example, the *Handbook of Chemistry and Physics*, The Chemical Rubber Co.

[23] I. Simon, A. G. Emslie, P. F. Strong, and R. K. McConnell, Jr., "Sensitive tiltmeter utilizing a diamagnetic suspension", *The Review of Scientific Instruments*, **39**, 1666–1671, (1968).

[24] R. D. Waldron, "Diamagnetic levitation using pyrolytic graphite", *The Review of Scientific Instruments*, **37**, 29–35, (1966).